A&A manuscript no.
(will be inserted by hand later)

Your thesaurus codes are:
06 (08.01.1 08.16.4 08.02.5 08.05.3 08.12.1)

ASTRONOMY AND ASTROPHYSICS

The Henize sample of S stars

I. The technetium dichotomy*

S. Van Eck and A. Jorissen **

Institut d'Astronomie et d'Astrophysique (IAA), Université Libre de Bruxelles, C.P.226, Boulevard du Triomphe, B-1050 Bruxelles, Belgium
email: svaneck@astro.ulb.ac.be, ajorisse@astro.ulb.ac.be

Received date; accepted date

Abstract. This paper is the first one in a series investigating the properties of the S stars belonging to the Henize sample (205 S stars with $\delta < -25°$ and $R < 10.5$) in order to derive the respective properties (like galactic distribution and relative frequencies) of intrinsic (i.e. genuine asymptotic giant branch) S stars and extrinsic (i.e. post mass-transfer binary) S stars. High-resolution (R=30 000 to 60 000) spectra covering the range $\lambda\lambda$4230−4270Å have been obtained for 76 S stars, 8 M stars and 2 symbiotic stars.

The λ4262Å and λ4238Å blends involving a Tc I line were analysed separately and yield consistent conclusions regarding the presence or absence of technetium. Only one 'transition' case (Hen 140 = HD 120179, a star where only weak lines of technetium are detectable) is found in our sample. A resolution greater than R = 30 000 is clearly required in order to derive unambiguous conclusions concerning the presence or absence of technetium. The Tc/no Tc dichotomy will be correlated with radial velocity and photometric data in a forthcoming paper.

Key words: Stars: late-type – Stars: AGB and post-AGB – Stars: evolution – Stars: abundances – binaries: symbiotic

1. Introduction

S stars have been identified as a class of peculiar red giants by Merrill (1922). Basically, the S stars emerge as a sequence parallel to the M stars as far as temperature is concerned, but with enhanced abundances of s-process elements. The chief observational difference between M and S spectra is the presence of ZrO bands in the latter. The s-process overabundances in S stars are explained in the framework of the Thermally Pulsing Asymptotic Giant Branch (TPAGB) evolution. Thermal instabilities (called *thermal pulses*) that affect the helium-burning shell of these stars have two important consequences: they provide the proper environment for the nucleosynthesis of s-process elements, and they trigger an envelope response (the *third dredge-up*) that allows the s-process elements and carbon to be brought to the surface [see e.g. Mowlavi (1997) for a review].

Technetium is an s-process element with no stable isotope that was first identified in the spectra of some M and S stars by Merrill (1952). ^{99}Tc, with a laboratory half-life of $t_{1/2} = 2.13 \times 10^5$ yr, is the only technetium isotope produced by the s-process. The high temperatures encountered during thermal pulses strongly shorten the effective half-life of ^{99}Tc ($t_{1/2} \sim 1$ yr at $\sim 3 \times 10^8$ K, Cosner et al. 1984) but the large neutron densities at these high temperatures more than compensate the reduction of ^{99}Tc lifetime (Mathews et al. 1986) and enable a substantial technetium production. Third dredge-up episodes then carry technetium to the envelope, where it decays steadily at its terrestrial rate of $t_{1/2} = 2.13 \times 10^5$ yr. Starting from an abundance corresponding to the maximum observed one, technetium should remain detectable during $1.0-1.5 \times 10^6$ yr (Smith & Lambert 1988). If the dredge-up of heavy elements occurs after each thermal pulse (occurring every $\sim 1-3 \times 10^5$ yr), virtually all s-process enriched TPAGB stars should exhibit technetium lines.

However, Straniero et al. (1995) advocated that the s-process nucleosynthesis solely occurs during the interpulse. When technetium is engulfed in the subsequent thermal pulse, it will decay at a fast rate because of the high temperature, and will not be replenished if there is no neutron source operating within the pulse itself. The conclusion that s-process enriched TPAGB stars should necessarily exhibit technetium would then be challenged. Nevertheless, all the S stars identified as TPAGB stars by Van Eck et al. (1998) thanks to the HIPPARCOS paral-

Send offprint requests to: S. Van Eck

* Based on observations carried out at the European Southern Observatory (ESO, La Silla, Chile)

** Research Associate, National Fund for Scientific Research (FNRS), Belgium laxes turned out to be Tc-rich. A survey of technetium in a large sample of S stars like the Henize sample may be expected to provide further constraints on the s-process environment in AGB stars (e.g. interpulse s-process versus thermal-pulse s-process, thermal-pulse duration and temperature versus ^{99}Tc half-life).

Not all S stars exhibit Tc lines though (Little-Marenin & Little 1979, Little et al. 1987), but technetium-poor stars (also called *extrinsic*, as opposed to technetium-rich, *intrinsic* S stars) are currently believed to emerge from a totally different evolutionary history: because they are members of binary systems (Brown et al. 1990, Jorissen et al. 1993, Johnson et al. 1993, Jorissen et al. 1998), they rather owe their chemical peculiarities to the accretion of s-process-rich matter from their companion (formerly a TPAGB star, now an undetected white dwarf). They are technetium-poor, because enough time has elapsed for the technetium to decay since the mass transfer event. The ^{99}Tc half-life is indeed much shorter than any stellar evolutionary timescale (but the TPAGB). Such a polluted giant star will be classified either as a G or K giant with enhanced heavy elements (i.e. as a barium star) or, if it has cooled enough for the ZrO molecular bands to appear, as a technetium-poor S star.

Besides technetium detection, several spectroscopic criteria (of various efficiencies) aiming at distinguishing extrinsic from intrinsic S stars have been mentioned in the literature [e.g. oxygen isotopic ratio (Smith & Lambert 1990), presence of the He I λ10830 line (Brown et al. 1990), zirconium isotopic ratio (Busso et al. 1992)], but technetium detection appears to be, by far, the most secure and tractable way to unmask extrinsic S stars.

This unmasking operation is crucial when deriving fundamental stellar quantities such as the third dredge-up luminosity threshold (commonly measured as the minimum luminosity of S stars). Evolutionary timescales of TPAGB stars can be strongly in error if the considered star samples are polluted by non-AGB, mass-transfer S stars.

We therefore decided to study a large and properly defined sample of S stars in order to disentangle the two sub-families and to study their respective characteristics. The Henize sample of S stars (Henize 1960, as listed in Stephenson 1984) consists of 205 S stars south of $\delta = -25°$ and brighter than $R = 10.5$. Radial velocity data, low- and high-resolution spectroscopy, as well as Geneva photometry have been collected over several years. The present paper deals with high-resolution technetium spectra for 72 Henize stars. Some additional K, M and symbiotic star data are also presented. Results concerning binarity and photometry, as well as the global analysis of the different data sets, are postponed to a forthcoming paper.

2. Observations and reductions

2.1. Instrumental set-up

The high-resolution spectra used in the present study were obtained during several runs (1991-1998) at the European Southern Observatory, with the Coudé Echelle Spectrometer (CES) fed by the 1.4m Coudé Auxiliary Telescope (CAT). The 1991-1993 runs were performed with the short camera (f/1.8) and CCD #9 (RCA SID 503 thinned, backside illuminated, 1024×640 pixels of 15 μm), whereas the long camera (f/4.7) and CCD #38 (Loral/Lesser thinned, backside illuminated, UV flooded, 2688×512 pixels of 15 μm) were used during the 1997-1998 runs. Details on these configurations can be found in Lindgren & Gilliotte (1989) and Kaper & Pasquini (1996). The resolution ranges from 0.14Å (R=30 000) to 0.07Å (R=60 000) for a central wavelength of 4250Å. The spectra approximately cover the wavelength range $\lambda\lambda$ 4230-4270Å.

2.2. Stellar samples

The observed stars are a subset of the sample of 205 S stars collected by Henize (1960) from his objective-prism survey (with a dispersion of 450Å/mm at Hα) of ZrO stars south of $\delta = -25°$ and brighter than $R = 10.5$. Given the limitations on the CAT pointing and on the detectors sensitivity, only stars with $\delta > -75°$, $V < 11$ and $B - V < 2$ (translating into 70 objects) could be observed in a reasonable amount of time, i.e. less than 1h30 per star. A few bright redder stars could also be observed (but see the discussion on SC stars in Sect. 3.2). A sample of bright M stars with an excess at 60μm [indicative of a possibly detached dust shell; see Zijlstra et al. (1992)], as well as the two symbiotic stars RW Hya and SY Mus, and some radial-velocity standards have also been observed. Three non-Henize S stars from our radial-velocity monitoring (Udry et al. 1998) have been included as well. The log of the observations, including the instrumental setting, is given in Table 1 and, for Henize stars, in Table 2.

2.3. Data reduction and S/N ratio

The CCD frames were corrected for the electronic offset (bias) and for the relative pixel-to-pixel response variations (flat-field). Wavelength calibration was performed from thorium lamp spectra taken several times per night. An optimal extraction of the spectra was performed according to the method of Horne (1986). The whole reduction sequence was performed within the 'long' context of the MIDAS software package.

The signal-to-noise (S/N) ratio was estimated for each spectrum in the following way: three S/N values were computed for the three best exposed CCD lines (along the dispersion axis), in the neighborhood of the spectral region

Table 1. Observations log and results for non-Henize stars.
The first column identifies the star by its HD, HR or BD number. The spectral type is quoted next. The next two columns list the civil date of the observation (day month year) and the Julian date (JD - 2 448 000.5). The column CCD provides the instrumental setting (9-sh: CCD #9 + short camera; 38-l: CCD #38 + long camera). The next column indicates the spectral resolution. The next six columns give, for the two considered technetium blends (at 4262Å and 4238Å, respectively), the (Doppler-shift corrected) central wavelength of the technetium blend (λ - 4200Å), the standard deviation on the Doppler shift (σ, in Å) and the signal-to-noise ratio (see text). The technetium-rich (y) or technetium-poor (n) status is given next, while the last column contains additional remarks

HD/BD	type	cdate	Jdate	CCD	R	4262Å blend			4238Å blend			Tc	Remarks
						λ	σ	S/N	λ	σ	S/N		
• M stars													
HR 4938	M3.5III	160393	1063.3	9-sh	45000	62.104	0.012	41	38.366	0.028	29	n	V789 Cen
HR 5064	K5-M0III	150393	1062.3	9-sh	45000	62.097	0.010	76	38.353	0.030	61	n	
HR 5134	M5III	150393	1062.3	9-sh	45000	62.069	0.015	70	38.356	0.037	53	n	V744 Cen
• M stars with 60μm excess													
73341	M3/M4III	300593	1138.0	9-sh	45000	62.103	0.011	33	38.370	0.030	25	n	SAO 236108
91094	M1III	300593	1138.0	9-sh	45000	62.099	0.014	39	38.357	0.025	34	n	SAO 250981
179199	M2III	290593	1137.4	9-sh	45000	62.097	0.017	18	38.354	0.032	15	n	SAO 162305
181620	M2III	290593	1137.4	9-sh	45000	62.109	0.016	29	38.368	0.025	23	n	V4415 Sgr;SAO 211215
• Symbiotic stars													
100336	M4.5	160393	1063.2	9-sh	45000	62.094	0.020	11	38.347	0.029	8	n	SY Mus
117970	M2	150393	1062.2	9-sh	45000	62.115	0.011	31	38.363	0.042	24	n	RW Hya
• Non-Henize S stars													
1760	M5-6Se	300792	834.4	9-sh	30000	62.230	0.020	65	38.142	0.030	55	y	T Ceti (also M5-6Ib-II)
−21°2601	S3*3	310197	2480.2	38-l	60000	62.097	0.007	22	38.365	0.024	16	n	
−08°1900	S4/6	240298	2869.0	38-l	60000	62.239	0.029	15	38.256	0.035	11	y	
+04°4356	S4*3	290593	1137.3	9-sh	45000	62.210	0.015	19	38.079	0.033	11	y	see note
• Radial velocity standards													
80170	K5III	240298	2869.1	38-l	60000	62.099	0.011	84	38.356	0.018	66	n	
108903	M3.5III	240298	2869.3	38-l	60000	62.104	0.012	233	38.372	0.016	182	n	γ Cru A

Note: The S star BD+04°4356 = GCGSS 1193 = SAO 125493 = IRAS 20062+0451 has been erroneously associated by MacConnell (1982) with the nearby (non-S) star BD+04°4354. The coordinates in the original paper are nevertheless correct. Since then, this error has propagated in the literature (Stephenson 1984, Jorissen et al. 1993, Chen et al. 1995, Jorissen et al. 1998, Udry et al. 1998), although in all these papers the measured star was indeed the S star BD+04°4356.

of interest (either 4262Å or 4238Å). These three S/N values were then combined according to Eq. 17 of Newberry (1991). When the exposure time on a given star has been split in two (in order to reduce cosmics detrimental effect), the final S/N ratio was computed using Eq. 18 of Newberry (1991). The degradation of the S/N ratio due to flat-field correction has not been taken into account, since flat-fields have little degrading effect for the low S/N values under consideration. The S/N ratio values are listed in Tables 1 and 2 for each target star. Because of the CCD spectral response, the S/N ratio near 4238Å is systematically lower than the one near 4262Å.

3. Analysis

3.1. Fit of the technetium blends

The three strong resonance lines of Tc I are located at 4238Å, 4262Å and 4297Å, with intensity ratios of 3:4:5. All three lines are severely blended (Little-Marenin & Little 1979, their Table III). With the adopted instrumental configurations, a single exposure spans 35 to 50Å; it is thus possible to observe simultaneously the 4238Å and 4262Å lines. In this analysis we follow the guidelines provided in the landmark paper of Smith & Lambert (1988) and therefore concentrate on the most useful 4262Å line, while the 4238Å line is used as an independent confirmation.

Fig. 1 shows examples of spectra in the 4262Å region for an M3-4 giant (HD 73341) and for seven S stars (four being technetium-poor: Hen 3, 187, 31, 7 and three technetium-rich: Hen 140, 39 and 202 = π^1 Gru). It can be seen that the Tc λ4262.270Å line is blended with two features; the bluest includes primarily Nb I (4262.050Å) and Gd II (4262.087Å), and the reddest Cr I (4262.373Å) (see Fig. 1). A weaker contribution of Nd II at 4262.228Å, almost on the top of the Tc I line, may also be present. These composite features are much weaker than the Tc I resonance line at its maximum strength; moreover, the Nb I-Gd II blend and the Tc I line are 0.18Å apart. Therefore the shape and location of the Nb I-Gd II (-Tc I) blend (hereafter called X_{4262} feature) clearly depends on whether it contains the technetium line or not. Quantitatively, the

Table 2. Same as Table 1 but for Henize S stars. The Henize and GCGSS numbers (Stephenson 1984) are listed in the first two columns. Spectral types are from Stephenson (1984)

Hen	GC-GSS	HD/DM	type	cdate	Jdate	CCD	R	4262Å blend			4238Å blend			Tc	Remarks
								λ	σ	S/N	λ	σ	S/N		
1	3	310	S3,1	210991	521.2	9-sh	30000	62.107	0.008	36	38.375	0.013	34	n	
2	39	9810	S2,1	210991	521.3	9-sh	30000	62.094	0.015	21	38.372	0.014	18	n	
3	104	29704	S:	210991	521.3	9-sh	30000	62.088	0.019	26	38.396	0.016	23	n	
5	139		S3,3	010297	2481.0	38-l	60000	62.089	0.007	18	38.394	0.010	12	n	
6	141		S5,2	300197	2479.1	38-l	60000	62.091	0.008	22	38.379	0.015	11	n	
7	178	40706	S2,1	150393	1062.0	9-sh	45000	62.126	0.022	22	38.367	0.025	20	n	
8	202	−39°2449	S5,6	010297	2481.1	38-l	60000	62.227	0.020	18	38.194	0.042	14	y	
9	204	−60°1381	S3,3	160393	1063.0	9-sh	45000	62.099	0.008	16	38.349	0.024	13	n	
14	242	−34°3019	S2,5	160393	1063.1	9-sh	45000	62.104	0.004	13	38.363	0.023	10	n	
16	248		S:	310197	2480.2	38-l	60000	62.258	0.019	13	38.172	0.014	7	y	
18	294	−28°3719	S6,8e	150393	1062.0	9-sh	45000	62.072	0.032	13	38.378	0.033	10	n	
19	328			310197	2480.1	38-l	60000	62.229	0.015	16	38.233	0.021	12	y	
20	342	−45°3132		310197	2480.0	38-l	60000	62.230	0.016	27	38.120	0.017	16	y	
28	390	62340	S4,4	010297	2481.1	38-l	60000	62.079	0.016	36	38.381	0.011	26	n	
31	434	65152	S1,1	150393	1062.1	9-sh	45000	62.093	0.009	31	38.369	0.026	27	n	
34	446		S7,2	010297	2481.1	38-l	60000	62.254	0.022	39	38.193	0.013	30	y	X Vol
35	447	−71°435	S1,1	300197	2479.1	38-l	60000	62.078	0.010	19	38.375	0.026	11	n	
36	448	−31°5393	S3,1	150393	1062.1	9-sh	45000	62.222	0.011	22	38.141	0.028	17	y	
37	456	−41°3702	S4,2	010297	2481.2	38-l	60000	62.260	0.004	19	38.090	0.017	12	y	
39	461	−65°601	S6,2	010297	2481.2	38-l	60000	62.238	0.004	31	38.118	0.014	21	y	
41	474	−27°5131	S4,2	010297	2481.2	38-l	60000	62.219	0.027	31	38.210	0.019	23	y	
43	487	−26°5801	S4,4	240298	2869.1	38-l	60000	62.099	0.012	15	38.348	0.026	10	n	
45	490	−32°5117		010297	2481.3	38-l	60000	62.212	0.015	25	38.147	0.019	18	y	
57	559		S4,2	310197	2480.2	38-l	60000	62.221	0.021	21	38.145	0.019	14	y	
63	588	−33°5772	S4,1	300197	2479.2	38-l	60000	62.103	0.013	15	38.364	0.017	10	n	
64	591	−28°6970	S7/5e	010297	2481.3	38-l	60000	62.252	0.010	17	38.181	0.031	7	y	
66	593	−33°5803	S5,2	310197	2480.3	38-l	60000	62.226	0.029	18	38.138	0.013	12	y	
79	653		S5,2	240298	2869.2	38-l	60000	62.097	0.011	19	38.388	0.023	14	n	
80	656		S5,6	150393	1062.2	9-sh	45000	62.254	0.017	15	38.138	0.022	12	y	KN Car
88	667	−30°8296	S5,2	300197	2479.3	38-l	60000	62.220	0.012	15	38.122	0.008	10	y	
89	668		S3,1	300197	2479.3	38-l	60000	62.223	0.018	18	38.091	0.012	9	y	
90	672	−54°3378	S5,6	240298	2869.2	38-l	60000	62.083	0.008	22	38.372	0.021	16	n	
95	693		S4,2	300593	1138.0	9-sh	45000	62.229	0.016	12	38.138	0.020	8	y	
97	696		S5,2	290593	1137.1	9-sh	45000	62.224	0.006	21	38.148	0.033	16	y	HP Vel
101	704		S5,4	240298	2869.3	38-l	60000	62.247	0.037	21	38.165	0.032	15	y	Z Ant
104	714	95013	S5,4	300593	1138.1	9-sh	45000	62.208	0.015	10	38.176	0.008	6	y	
108	720	95875	S3,3	300197	2479.3	38-l	60000	62.087	0.014	34	38.368	0.017	21	n	
119	778	104361	S3,3	010297	2481.4	38-l	60000	62.084	0.010	27	38.377	0.015	16	n	
121	792	−27°8661	S4,6e	300593	1138.1	9-sh	30000	62.098	0.016	10	38.374	0.035	8	n	
123	795	−47°7642	S4,2	160393	1063.3	9-sh	45000	62.096	0.013	20	38.358	0.027	14	n	CSV101280
126	802		S4,2	240298	2869.4	38-l	60000	62.100	0.018	17	38.368	0.022	12	n	
129	808	−46°8238	S4,4	290593	1137.1	9-sh	45000	62.073	0.018	14	38.384	0.034	11	n	
132	813	−72°869	S4,6	300593	1138.2	9-sh	30000	62.081	0.011	12	38.355	0.038	9	n	
133	814	114586	S5,4	240298	2869.3	38-l	60000	62.073	0.008	20	38.367	0.021	16	n	
137	824	−50°7894		160393	1063.3	9-sh	45000	62.088	0.013	22	38.366	0.028	14	n	
138	826	118685	S6,2	150393	1062.3	9-sh	45000	62.092	0.008	32	38.367	0.027	25	n	-71 963
140	832	120179	S3,1	310197	2480.3	38-l	60000	–	–	36	–	–	27	y	see text
140	832	120179	S3,1	300593	1138.2	9-sh	30000	–	–	26	–	–	20	y	see text
141	834	120460	S8,5	230597	2592.2	38-l	60000	62.250	0.044	19	38.181	0.018	12	y	VX Cen
143	839	122434	S3,1	010297	2481.4	38-l	60000	62.092	0.013	27	38.372	0.019	19	n	-41 8409
147	858	−25°10393	S3,3	290593	1137.2	9-sh	45000	62.084	0.024	9	38.356	0.015	7	n	
149	864	130859	S4,2	150393	1062.4	9-sh	45000	62.102	0.007	13	38.370	0.023	10	n	
150	867	131217	S6,2	010892	836.0	9-sh	30000	62.093	0.012	6	38.376	0.037	5	n	
162	927		S5,2	300593	1138.3	9-sh	30000	62.239	0.016	18	38.181	0.039	14	y	
173	962		S4,2	300593	1138.3	9-sh	30000	62.096	0.015	9	38.336	0.044	7	n	
175	974	156957	S6/3+	310792	835.1	9-sh	30000	62.243	0.032	21	38.142	0.027	16	y	V635 Sco
177	977	−32°12687	S:	230597	2592.4	38-l	60000	62.232	0.032	24	38.107	0.027	12	y	
178	978	157335	S5,4	300593	1138.4	9-sh	30000	62.272	0.020	10	38.118	0.049	6	y	V521 Oph
179	994	160379	S5,2	150393	1062.4	9-sh	45000	62.090	0.012	17	38.369	0.025	13	n	
182	1010	163896	S4,2	310792	835.2	9-sh	30000	62.082	0.008	25	38.376	0.027	22	n	V745 Sgr
183	1014	164392		310792	835.1	9-sh	30000	62.089	0.013	26	38.369	0.029	22	n	
186	1023	165774	S4,6	210991	521.0	9-sh	30000	62.090	0.011	30	38.375	0.012	26	n	
187	1025	165843	S2,1	300593	1138.4	9-sh	30000	62.084	0.014	20	38.388	0.038	14	n	
191	1056	171100	S5,4	310792	835.2	9-sh	30000	62.244	0.021	19	38.166	0.035	15	y	V3574 Sgr
193	1074	−23°14695	S4,2	300792	834.2	9-sh	30000	62.106	0.006	9	38.344	0.018	8	n	
197	1195	191630	S4,4	210991	521.0	9-sh	30000	62.216	0.014	50	38.147	0.011	42	y	
199	1212			310792	835.3	9-sh	30000	62.094	0.013	14	38.363	0.021	12	n	
201	1275	−26°15676	S3,3	300792	834.3	9-sh	30000	62.098	0.013	15	38.366	0.045	13	n	
202	1294		S5,7:	210991	521.1	9-sh	30000	62.270	0.034	27	38.191	0.011	17	y	π^1 Gru
203	1295		S4,4	300792	834.3	9-sh	30000	62.067	0.017	12	38.358	0.033	12	n	
204	1303		S6,6	310792	835.3	9-sh	30000	62.116	0.016	19	38.368	0.023	17	n	CSV103101

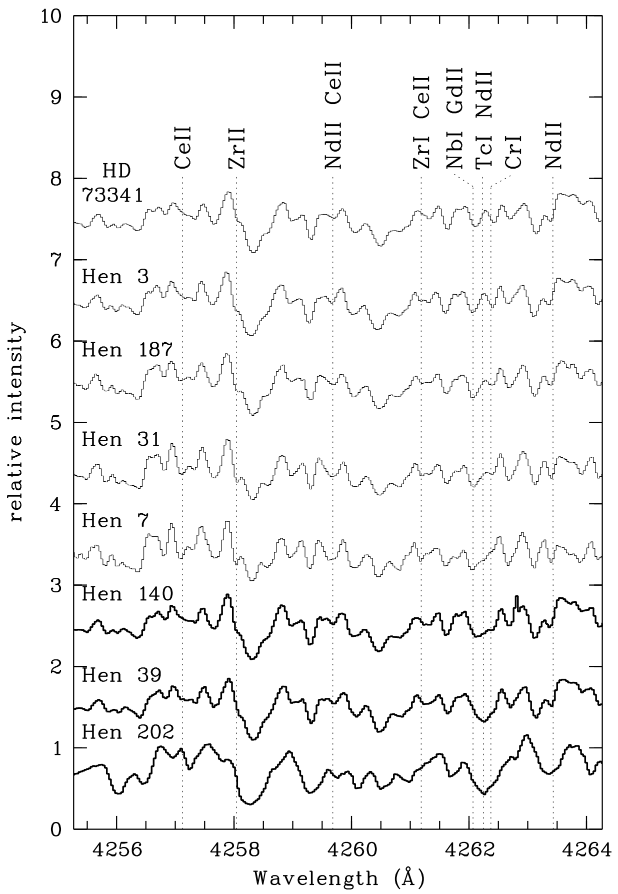

Fig. 1. Spectra in the 4262Å region. The top spectrum is HD 73341, a normal giant (M3/M4III); the other spectra correspond to Henize S stars. Technetium-poor spectra are plotted with a thin line; technetium-rich spectra with a thick line. Hen 3, 187, 31, 7 are typical Tc-poor stars; Hen 39 and 202 are typical Tc-rich stars. The Tc-rich spectrum of Hen 140 is unique in our sample and remarkable because of its very weak Tc lines (see Sect. 3.1). All spectra are plotted on the same relative intensity scale. The local pseudo-continuum point has been taken as an average of the fluxes at 4239.1, 4244.1, 4247.1 and 4265.4Å; for the sake of clarity, each spectrum (except the lowest one) is vertically shifted by 1 unit with respect to the spectrum below it. Some spectral features of s-process elements are identified (see text)

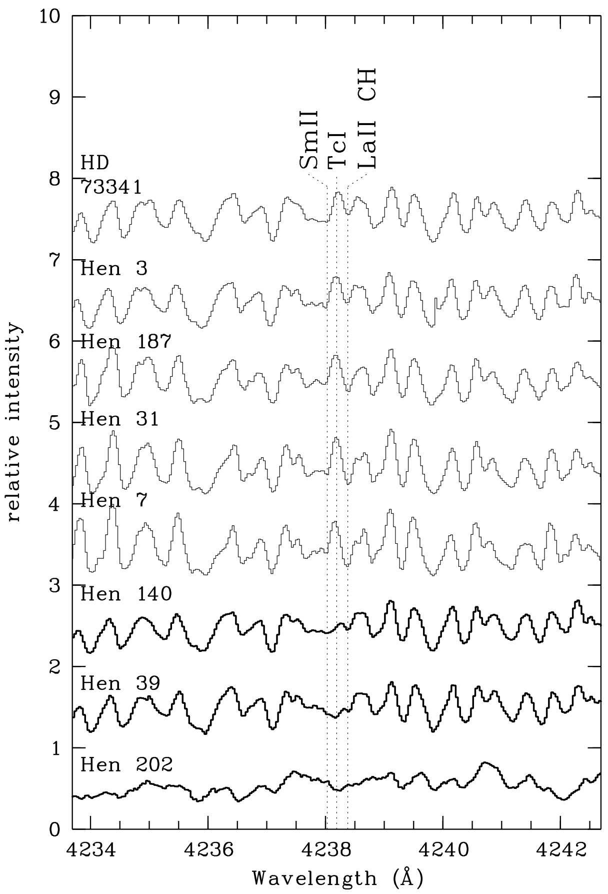

Fig. 2. Same as Fig. 1 for the 4238Å region

minimum of a gaussian fitted to a Tc-containing X_{4262} feature is shifted redward by ~ 0.14Å with respect to the minimum of a gaussian fitted to a no-Tc X_{4262} feature; such a shift is easily detectable on our spectra (compare Hen 3 or Hen 7 with Hen 39 on Fig. 1).

In practice, each spectrum has been rebinned to zero-redshift in the following way: 10 nearby (≤ 5Å on either side) apparently unblended stellar features with unambiguous identification, are adopted as wavelength standards. Gaussian profiles are fitted to these lines and provide a mean redshift. The wavelength of the X_{4262} feature is then computed as the minimum of a gaussian centered on the X_{4262} feature of the redshift-corrected spectrum. Typical uncertainties on the X_{4262} wavelength amount to 0.013Å for technetium-poor stars and 0.020Å for technetium-rich stars (as derived from the standard deviation on the mean redshift).

The same method is applied to the 4238Å technetium line, where the CH-La II blend has been taken as the X_{4238} feature (Fig. 2). Typical uncertainties on the X_{4238} wavelength are slightly larger (0.023Å for Tc-rich S stars and 0.025Å for Tc-poor S stars) because of the lower S/N ratio and the stronger blending at 4238Å. Results are listed in Tables 1 and 2; the X_{4238} and X_{4262} features always yield consistent results regarding the absence or presence of technetium, except for Hen 140 (=HD 120179).

This star is indeed unique in having very weak technetium features (see Figs. 1 and 2). A second spectrum, taken 3.5 years later, is almost identical to the one displayed in Fig. 1 and 2. The blind application of gaussian fitting to the X_{4238} feature of Hen 140 yields a central wavelength that would qualify it as Tc-poor; however, the extreme weakness of the pseudo-emission separating the LaII-CH blend from the SmII line as seen in Hen 140

(Fig. 2) is unusual for Tc-poor stars, and suggest the presence of a weak technetium line, as confirmed from the appearance of the X_{4262} feature. We therefore believe that Hen 140 is the unique example in our sample of an S star with very weak Tc lines.

In all the other cases, technetium (non-) detection relies on the location of the minimum of a gaussian fitted to the X_{4262} (or X_{4238}) blend.

Are there, with this method, risks (i) to misclassify as Tc-rich a truly Tc-poor star, and (ii) to misclassify as Tc-poor a truly Tc-rich star? We show in the remaining of this section that both risks are most probably non-existent in the present study.

Error (i) could, in principle, affect very luminous Tc-poor stars, because their large macroturbulence would broaden their X_{4262} feature, which could then possibly mimick a Tc-rich feature.

In order to test this hypothesis, gaussian filters of different widths have been applied to Tc-poor spectra, so as to make their line widths comparable to those of the stars classified as Tc-rich. This simulation clearly shows that even the largest macroturbulence value observed in our sample (T Ceti) is not large enough to make truly Tc-poor stars appear as Tc-rich from the broadening of their X_{4262} feature. That conclusion is even more stringent when considering the X_{4238} feature. However, this risk cannot be excluded for very luminous stars (class I or II) if observed at lower resolution (R $<$ 30 000).

Error (ii) could, in principle, occur for stars displaying a 'weak technetium line' (weaker than the Tc lines of Hen 140 discussed above) with an intensity not large enough to shift the X_{4262} blend redward from the Tc-poor wavelength. In fact, some stars in our sample exhibit an 'ambiguous' X_{4262} blend, in the sense that the pseudo-emission located between the Nb I-Gd II lines and the Cr I line becomes very weak or even disappears, mimicking a 'weak technetium line' (a typical example is Hen 7 on Fig. 1). Such a star is classified by our method as technetium-poor, for the minimum of the X_{4262} blend remains unchanged with respect to the no-Tc cases.

In fact, all intermediates exist between the 'unambiguous' X_{4262} Tc-poor blends (with a clear central pseudo-emission, see HD 73341 and Hen 3 on Fig. 1) and the 'ambiguous' X_{4262} blends (where this pseudo-emission is absent, as in Hen 7); two typical transition cases are plotted on Fig. 1 (Hen 187 and Hen 31). These 'ambiguous' spectra were taken during different observing runs; the shape of the X_{4262} blend is independent of the resolution and of the S/N ratio of the spectra.

Do these 'ambiguous' spectra correspond to stars with a weak technetium line, intermediate between the clear Tc-poor and Tc-rich cases? In fact these 'ambiguous' spectra are clearly different from the spectum of the weakly Tc-rich star Hen 140, for *their* X_{4238} *feature is identical to the* X_{4238} *feature of the unambiguous Tc-poor stars* (Fig. 2), which clearly indicates that technetium is absent in these stars.

It may therefore be concluded that our method of gaussian fit to the X_{4238} and X_{4262} features is able to properly separate technetium-rich from technetium-poor S stars.

What then causes the variety of X_{4262} features observed in Fig. 1 for technetium-poor S stars? The spectral sequence going from Hen 3 to Hen 7 on Fig. 1 is not a temperature sequence. The temperature of the stars of our sample have been derived from the $V-K$ color index using the Ridgway et al. (1980) calibration, the K magnitudes from Catchpole et al. (1979) and our Geneva photometry. Although the bulk of technetium-rich S stars are clearly cooler than technetium-poor S stars (see also Van Eck et al. 1998), there is no sign whatsoever of a possible correlation between the shape of the X_{4262} blend of technetium-poor stars and their temperature. MOOG (Sneden 1974) synthetic spectra (for stars with $T_{\rm eff}\sim$ 3400−3800 K as derived from their $V-K$ index) indicate that neither gravity nor metallicity can significantly modify the X_{4262} blend.

A closer inspection of the spectral sequence of Fig. 1 (from HD 73341 to Hen 7) reveals that several lines become stronger as the central pseudo-emission of the X_{4262} blend weakens. The major contributors to these features, identified with the help of synthetic spectra, are indicated on the top of Fig. 1. It is noteworthy that *all these elements are s-process elements*. The sequence of spectra (drawn with a thin line) in Fig. 1 is thus, from top to bottom, a sequence of increasing s-process line strengths (s-process lines being weak, as expected, in the M star HD 73341). The line which progressively blends the X_{4262} feature of technetium-poor stars is thus probably an s-process line as well. Since it cannot be technetium (see above), a good candidate is the 4262.228Å line of Nd II, or perhaps the Gd II line at 4262.087Å.

It is not surprising to find a wide range of s-process enhancements among technetium-poor S stars, since these stars have accreted their s-process-enriched matter from a companion star. Hence the level of chemical peculiarities is not linked to the evolutionary status of the star, but rather depends upon the amount of s-process accreted matter (see Jorissen et al. 1998 for a detailed discussion).

These s-process lines are more difficult to see in the technetium-rich S stars, probably because in these cooler and more luminous stars, lines are broader (because of a larger macroturbulence) and the molecular blanketing is more severe.

3.2. Misclassified and SC stars

The method outlined in Sect. 3.1 cannot be applied to four stars of our sample which exhibit peculiar spectra (Hen 22, 135, 154 and 198). In order to check the assignment of the Henize stars to spectral type S, low-resolution spectra ($\Delta\lambda\sim$ 0.3 nm, 4400Å$<\lambda<$ 8200Å) have been

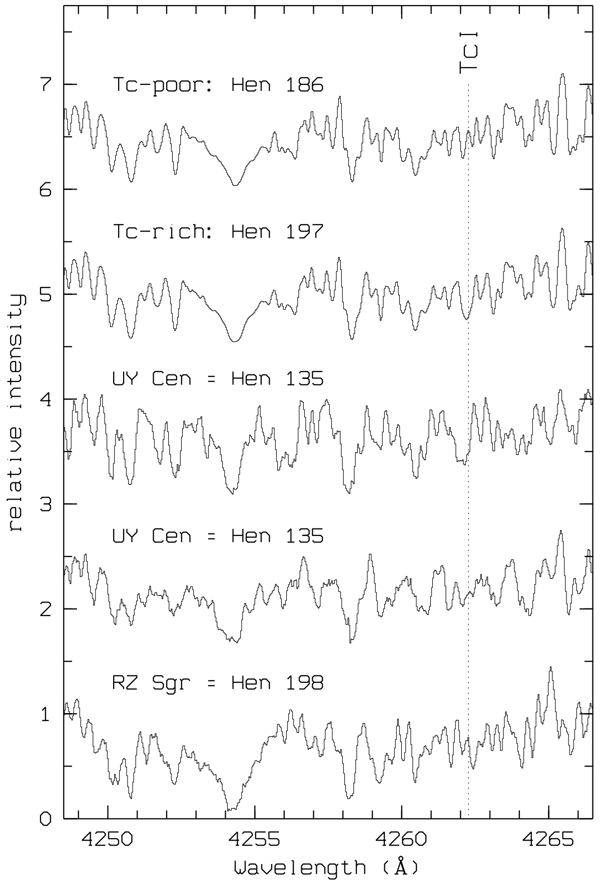

Fig. 3. Same as Fig. 1, but for two prototype S stars (Hen 186, Tc-poor and Hen 197, Tc-rich), and for the two outstanding stars UY Cen (SC) and RZ Sgr. Note the striking differences between the lower and upper spectra of UY Cen, taken on March 16, 1993 and on January 31, 1997, respectively. The local pseudo-continuum point is defined as in Fig. 1; for the sake of clarity, each spectrum (except the lowest one) is vertically shifted by 1.5 unit with respect to the spectrum below it

obtained for all stars from Hen 3 to Hen 165 at ESO on the 1.52m telescope equipped with the Boller & Chivens spectrograph and grating #23 (Van Eck et al. 1999).

Two misclassified stars have been uncovered: Hen 22 and Hen 154 show no sign of ZrO bands whatsoever in their spectra. Besides, Hen 22 is classified as 'S:' by Henize. Both stars cannot be dwarfs because their NaD and MgH λ4780Å features are too weak. Their prominent Ca I λ 4455Å line and their weak CN λ7895Å band point towards them being giant stars rather than supergiants. Type Ia supergiants can certainly be ruled out because their absolute magnitudes ($M_{\rm v} = -7.8$ and -7.5 for G8Ia and K3-5I respectively, Landolt-Börnstein 1982) would result in much too large heights above the galactic plane (7.5 kpc for Hen 154 and 13.2 kpc for Hen 22). Hen 154 is probably a late G giant (~G8), and Hen 22 a mid-K giant (~K3-5). These assignments are compatible with the Geneva photometry available for these two stars.

As far as Hen 135 and Hen 198 are concerned, Fig. 3 shows that the spectra of these stars are very different from those of other S stars of the Henize sample. Many spectral features adopted as wavelength standards, as well as the technetium blend, are difficult or even impossible to identify in the spectra of Hen 135 and Hen 198. In fact, we show below that these two stars are the only two SC stars in the subsample of Henize S stars observed with the CAT[1]. Hen 135 ($V \sim 7$) and Hen 198 ($V \sim 7-10$) were indeed the only very red stars ($B-V > 2$) which were bright enough to allow spectra to be taken in the violet.

SC stars are known to have very peculiar spectra. Their spectrum is filled with strong atomic lines and almost no molecular bands in the optical, a consequence of their C/O ratio being very close to unity (Scalo 1973). Catchpole & Feast (1971) define SC stars from the following three criteria: (i) extremely strong Na D lines, (ii) drop in the continuum intensity shortward of 4500Å, and (iii) bands of ZrO and CN simultaneously present (though quite weak), as well as general resemblance of the spectrum (i.e. regarding 'the absolute and relative strength of metal lines') with that of UY Cen.

Hen 135 (=UY Cen) is thus the prototype SC star. Our two spectra of that star (taken in March 1993 and January 1997, see Fig. 3) are quite different; in particular the shape of the X_{4262} feature has changed noticeably. Therefore it is hazardous to infer the technetium content of UY Cen from these data alone without the help of appropriate model atmospheres and synthetic spectra, which is beyond the scope of this paper.

Hen 198 (=RZ Sgr) has an Se-type spectrum; Stephenson (1984) quotes the HD catalogue noting that 'the spectrum is similar to class N, but does not belong to that class'. It is probably associated with a reflection nebula (Whitelock 1994). RZ Sgr is a large-amplitude (~ 2.5 mag) SRb-type variable ($P = 203.6$ d). Its Hα emission, as well as the TiO and ZrO band strengths, are variable. Catchpole & Feast (1976) also note that the Zr:Ti ratio of RZ Sgr is unusually high for an S star, and rather close to the one of N-type carbon stars.

Although RZ Sgr has not been classified as an SC star, it shares many common features with that family. Indeed, it reasonably meets the three criteria mentioned above for SC stars:
(i) Reid and Mould (1985) measured the strength of the Na D lines for several S, SC and C stars, including RZ Sgr. A spectrophotometric index of 1.07 is found for RZ Sgr, much larger than typical values for S stars (0.22 for BD+28°4592 and 0.28 for NQ Pup), but comparable to values obtained for SC stars (0.55 for LMC 441, 1.73 for

[1] Although the Henize sample contains several SC stars, they are usually too red, hence too faint at 4250Å, to be observed with the CAT.

R CMi, 2.57 for VX Aql). Thus RZ Sgr has abnormally strong Na D lines with respect to other S stars.
(ii) The ultraviolet flux deficiency of SC stars is clearly apparent from photometric data in the Geneva system. Indeed, the mean wavelengths of the B and V filters are $\lambda_0(B) = 4227$Å and $\lambda_0(V) = 5488$Å (Rufener & Nicolet 1988); therefore the $B - V$ index is highly sensitive to the ultraviolet flux deficiency of SC stars occurring for $\lambda < 4500$Å. SC stars have $B - V > 2$, whereas the bulk of S stars have $B - V < 2$. In that respect again, RZ Sgr ($2.0 < B - V < 3.0$) is typical of SC stars.
(iii) ZrO is present (although weak) in RZ Sgr; we found no information about the possible presence of CN bands. Infrared CO bands are stronger in RZ Sgr than in many other S and SC stars (Whitelock et al. 1985), probably locking a great quantity of carbon.

The IRAS colours of RZ Sgr also share many similarities with SC stars: it is located in a region of the (K − [12],[25] − [60]) color-color diagram ('region E' as defined by Jorissen & Knapp 1998) containing mainly SC stars with large 60μm excess and often resolved shells (see also Young et al. 1993).

All these arguments therefore indicate that RZ Sgr is closely related to the SC family. As pointed out for UY Cen, the 4262Å and 4238Å lines of Tc I are very difficult to analyse in SC stars. An assignment of these two stars to either the Tc-rich or Tc-poor group has therefore not been attempted here. Abia & Wallerstein (1998) nevertheless suggest that SC stars are Tc-rich, based on a quantitative analysis.

4. Discussion

4.1. The technetium dichotomy

The lower part of Fig. 4 shows the frequency histogram of the wavelength of the X_{4262} spectral feature for stars of Tables 1 and 2. The stars of our sample clearly segregate in two groups. The average wavelength of the bluer group is 4262.093Å; this group thus corresponds to Tc-poor S stars. The average wavelength of the redder group is 4262.235Å, thus revealing the contribution of the Tc I 4262.270Å line to the Gd II-Nb I blend. The standard deviation on the X_{4262} wavelengths is 0.012Å for Tc-poor stars and 0.017Å for Tc-rich stars. These values are in good agreement with the estimated errors on the X_{4262} wavelength (0.013Å for Tc-poor and 0.020Å for Tc-rich stars, Sect. 3.1).

The two groups are clearly separated by a 0.08Å gap, *with no intermediate cases.* Therefore, in order to distinguish Tc-poor from Tc-rich stars (on our spectra of resolution in the range 30 000-60 000), a delimiting wavelength of 4262.16Å may be safely adopted.

A similar conclusion holds for the X_{4238} feature (Fig. 5), where a boundary wavelength of 4238.29Å unambiguously

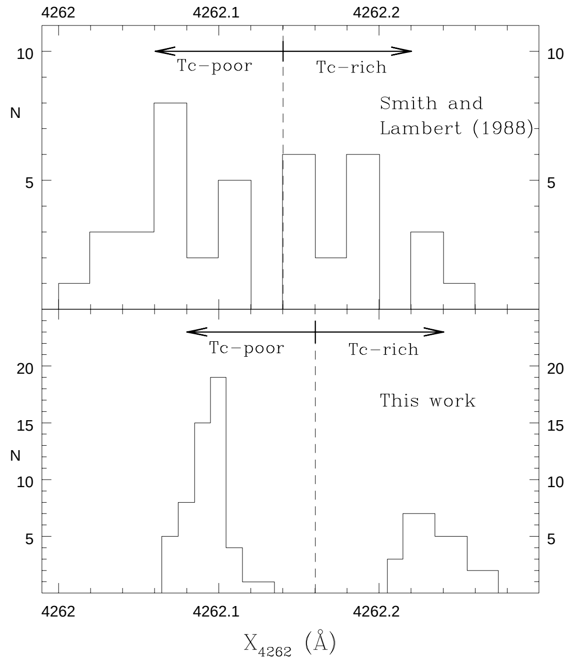

Fig. 4. Frequency histograms of the wavelength of the X_{4262} spectral feature. Top: results of Smith & Lambert (1988) for their sample of MS and S stars; the dotted line delimits the boundary wavelength (4262.14Å) between Tc-poor and Tc-rich S stars, as adopted by Smith & Lambert (1988). Bottom: same for all stars of Tables 1 and 2, where the boundary wavelength has been taken at 4262.16Å

separates the two kinds of S stars. Fig. 5 further shows that the diagnostics provided by the X_{4238} and X_{4262} features are consistent with each other.

For comparison purpose the frequency histogram of the wavelength of the X_{4262} spectral feature as obtained by Smith & Lambert (1988) is plotted in the upper part of Fig. 4, for their sample of MS and S stars (their Table 2). The segregation into Tc-poor and Tc-rich S stars (with 4 stars falling on their boundary wavelength at 4262.14Å) is not as clean as with our higher resolution spectra.

The small number of 'transition stars' in our sample (i.e. stars with weak Tc lines, the only case being Hen 140) is noteworthy. This result may provide constraints on the evolution with time of the technetium abundance along the TPAGB (Smith & Lambert 1988; Busso et al. 1992) and clearly deserves further studies. For example, it would be of interest to investigate whether the small number of S stars with weak technetium lines found in our sample implies that the very first objects to dredge-up heavy elements on the TPAGB are not S stars but rather M stars. Indeed, the Tc detection threshold might not coincide with the ZrO detection threshold, but be slightly lower (i.e. *stars would appear Tc-rich before being ZrO-rich*); this would explain the puzzling Tc-rich M stars discovered by Little-Marenin (1979) and Little et al. (1987).

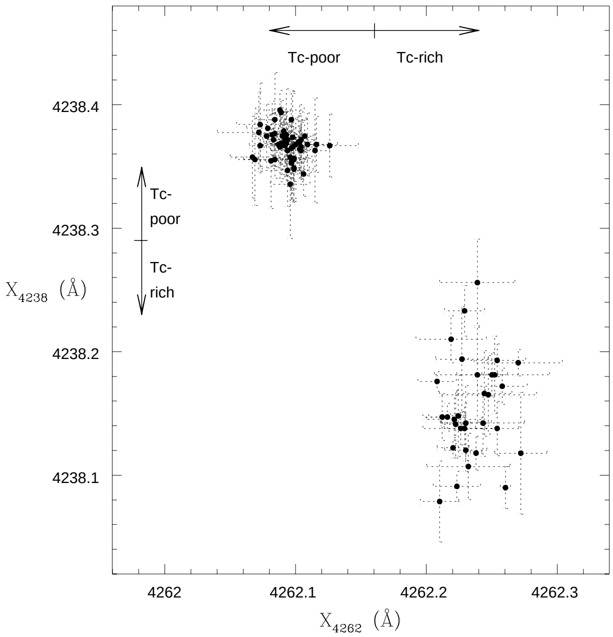

Fig. 5. The wavelength of the X_{4262} Tc feature versus the wavelength of the X_{4238} Tc feature. Errorbars represent the standard deviation of the mean redshift (computed from the ~10 spectral features adopted as wavelength standards). The technetium class (Tc-rich or Tc-poor) derived from the X_{4238} blend always confirms the technetium class derived from the X_{4262} blend; the Tc-poor and Tc-rich regions are clearly distinct. The boundary wavelengths adopted in this study between Tc-rich and Tc-poor stars are 4262.16Å for the X_{4262} feature (horizontal axis) and 4238.29Å for the X_{4238} feature (vertical axis); they are indicated by arrows

It is moreover necessary to disentangle abundance effects from atmospheric effects on the technetium line strength.

Although a more detailed study is deferred to a forthcoming paper, it may already be mentioned at this point that the Tc/no-Tc dichotomy reported in this paper is not due to technetium being entirely ionized in the warmer S stars. Indeed, the Tc I/(Tc I + Tc II) ratio is still ~ 40% in the warmest S stars ($T_{\rm eff}$=3800 K) while it amounts to ~ 70% at $T_{\rm eff}$=3500 K and to ~ 95% at $T_{\rm eff}$=3000 K, according to the Saha ionization equilibrium formula (with representative electron densities taken from model atmospheres).

4.2. M stars with 60μm excess and symbiotic stars

None of the four M stars with 60μm excess taken from the sample of Zijlstra et al. (1992) show technetium. This observation clearly indicates that these stars, which are surrounded by cool dust dating back to a former episode of strong mass loss, do not currently experience heavy elements synthesis followed by third dredge-ups. The same conclusion holds true for the two observed symbiotic stars (SY Mus and RW Hya).

5. Conclusion

High-resolution spectra have been obtained and analysed to infer the technetium content of 76 S, 8 M and 2 symbiotic stars. The presence or absence of technetium was deduced from the shape of two blends involving technetium at 4238Å and 4262Å (more precisely: from the wavelength of their minimum). However this method does not apply to SC stars. Two misclassified S stars (Hen 22 and Hen 154) have emerged. The technetium (non-)detection at 4238Å is consistent with the result at 4262Å. Only one 'transition' case (Hen 140 = HD 120179, a star where only weak lines of technetium are detectable) is found in our sample.

A resolution in excess of 30 000 is definitely required to provide unambiguous conclusions regarding presence or absence of technetium. For example, at 4262Å, an s-process line (possibly Nd II) is suspected to sometimes mimick a weak technetium line (although the 4238Å feature clearly shows that technetium is absent). The shape of the λ4262Å feature varies from one Tc-poor star to another, depending on the s-process overabundance level, which is in turn a function of the amount of accreted matter by these binary S stars.

Among the 70 analysed Henize S stars, 41 turn out to be technetium-poor and 29 technetium-rich. That fraction may not be used, however, to infer the relative frequencies of intrinsic and extrinsic S stars, since the subsample of Henize S stars observed with the CAT is biased towards the brightest and bluest stars. The frequency of extrinsic/intrinsic S stars will be derived from the whole data set in a forthcoming paper.

Acknowledgements. This research has made use of the Simbad database, operated at CDS, Strasbourg, France. S.V.E. thanks F.R.I.A. (Belgium) for financial support.

References

Abia C., Wallerstein G., 1998, MNRAS 293, 89

Brown J.A., Smith V.V., Lambert D.L., Dutchover E.Jr., Hinkle K.H., Johnson H.R., 1990, AJ 99, 1930

Busso M., Gallino R., Lambert D.L., Raiteri C.M., Smith V.V., 1992, ApJ 399, 218

Catchpole R.M., Feast M.W., 1971, MNRAS 154, 197

Catchpole R.M., Feast M.W., 1976, MNRAS 175, 501

Catchpole R.M., Robertson B.S.C., Lloyd Evans T.H.H., Feast M.W., Glass I.S., Carter B.S., 1979, Circulars of the South African Astronomical Observatory, Vol 1, Nr 4, p 61

Chen P.S., Gao H., Jorissen A., 1995, A&AS 113, 51

Cosner K.R., Despain K.H., Truran J.W., 1984, ApJ 283, 313

Horne K., 1986, PASP 98, 609

Johnson H.R., Ake T.B., Ameen M.M., 1993, ApJ 402, 667

Jorissen A., Frayer D.T., Johnson H.R., Mayor M., Smith V.V., 1993, A&A 271, 463
Jorissen A., Knapp G. R., 1998, A&AS 129, 363
Jorissen A., Van Eck S., Mayor M., Udry S., 1998, A&A 332, 877
Henize K.G., 1960, AJ 65, 491
Kaper L., Pasquini L., 1996, CAT+CES Operating Manual, ESO, 3p6CAT-MAN-0633-0001
Landolt-Börnstein, Numerical Data and Functional Relationships in Science and Technology, New Series, Hellwege ed., Astronomy and Astrophysics, vol 2, subvol b, 1982
Lindgren H., Gilliotte A., 1989, The Coudé Echelle Spectrometer, The Coudé Auxiliary Telescope, ESO Operating Manual No. 8
Little-Marenin I.R., Little S.J., 1979, AJ 84, 1374
Little S.J., Little-Marenin I.R., Hagen-Bauer W., 1987, AJ94, 981
MacConnell D.J., 1982, A&AS 48, 355
Mathews G.J., Takahashi K., Ward R.A., Howard W.M., 1986, ApJ 302, 410
Merrill P.W., 1922, ApJ 56, 457
Merrill P.W., 1952, ApJ 116, 21
Mowlavi N., 1997, in: Tours Symposium on Nuclear Physics III, eds. M. Arnould, M. Lewitowicz, Y.T. Oganessian, M. Ohta, H. Utsunomiya, T. Wada, AIP Conf. Proc. 425, p507
Newberry M.V., 1991, PASP 103, 122
Reid N., Mould J., 1985, ApJ, 299,236
Ridgway S.T., Joyce R.R., White N.M., Wing R.F., 1980, ApJ 235, 126
Rufener F., Nicolet B., 1988, A&A 206, 357
Scalo J.M., 1973, ApJ 186, 967
Sneden C., 1974, Ph. D. Thesis, University of Texas, Austin
Smith V.V., Lambert D.L., 1988, ApJ 333, 219
Smith V.V., Lambert D.L., 1990, ApJS 72, 387
Stephenson C.B., 1984, The General Catalogue of Galactic S Stars, Publ. Warner & Swasey Observ. 3,1
Straniero O., Gallino R., Busso M., Chiefei A., Raiteri C. M., Limongi M., Salaris M., 1995, ApJ 440, L85
Udry S., Mayor M., Van Eck S., Jorissen A., 1998, A&AS 131, 25
Van Eck S., Jorissen A., Udry S., Mayor M., Pernier B., 1998, A&A 329, 971
Van Eck et al., 1999, in preparation
Whitelock P., 1994, MNRAS 270, L15
Whitelock P., Catchpole R.M., 1985, MNRAS 212, 873
Young K., Phillips T.G., Knapp G.R., 1993, ApJS 86, 517
Zijlstra A.A., Loup C., Waters L.B.F.M., de Jong T., 1992, A&A 265, L5